

Electronic Supplementary Information:

The two new derivatives of scandium borohydride, $MSc(BH_4)_4$, $M = Rb, Cs$, prepared via a one-pot solvent-mediated method

A. Starobrat,^{a,b*} T. Jaroń^{b*} and W. Grochala^b

^a College of Inter-Faculty Individual Studies in Mathematics and Natural Sciences (MISMaP), University of Warsaw, Banacha 2c, 02-097 Warsaw, Poland

^b Centre of New Technologies, University of Warsaw, Banacha 2c, 02-097 Warsaw, Poland

Contents:

1. Figure S1. Rietveld plot of $CsSc(BH_4)_4$.
2. Figure S2. Rietveld plot of $RbSc(BH_4)_4$.
3. Figure S3. FTIR spectra of $CsSc(BH_4)_4$ samples.
4. Figure S4. FTIR spectra of $RbSc(BH_4)_4$ samples.
5. Figure S5. Sc-Rb zigzag lines in $RbSc(BH_4)_4$.
6. Figure S6. Mass spectrum of gaseous decomposition products of $RbSc(BH_4)_4$ obtained mechanochemically.
7. Figure S7. Mass spectrum of gaseous decomposition products of $RbSc(BH_4)_4$ obtained via DMS-mediated synthesis.
8. Figure S8. Mass spectrum of gaseous decomposition products of $CsSc(BH_4)_4$ obtained mechanochemically.
9. Figure S9. Mass spectrum of gaseous decomposition products of $CsSc(BH_4)_4$ obtained via DMS-mediated synthesis.
10. Figure S10. Crystal structure of M_3ScCl_6 , $M=Rb, Cs$ - the elpasolite-type structure.
11. Figure S11. PXRD patterns of $CsSc(BH_4)_4$ samples obtained via solvent-mediated and mechanochemical synthesis and by-products of solvent-mediated synthesis.
12. Figure S12. Rietveld plot of Cs_3ScCl_6 .
13. Figure S13. Rietveld plot of Rb_3ScCl_6 .
14. Figure S14. PXRD patterns of Rb-Y samples prepared via solvent-mediated method.
15. Figure S15. FTIR spectra of Rb-Y samples prepared via solvent-mediated method.
16. The structures of $MSc(BH_4)_4$ optimized computationally
17. Table S1. Comparison of the selected parameters for the experimental and computed structures.
18. Figure S16. An overlay of the experimental and computationally optimized structures of $RbSc(BH_4)_4$.
19. Figure S17. An overlay of the experimental and computationally optimized structures of $CsSc(BH_4)_4$.

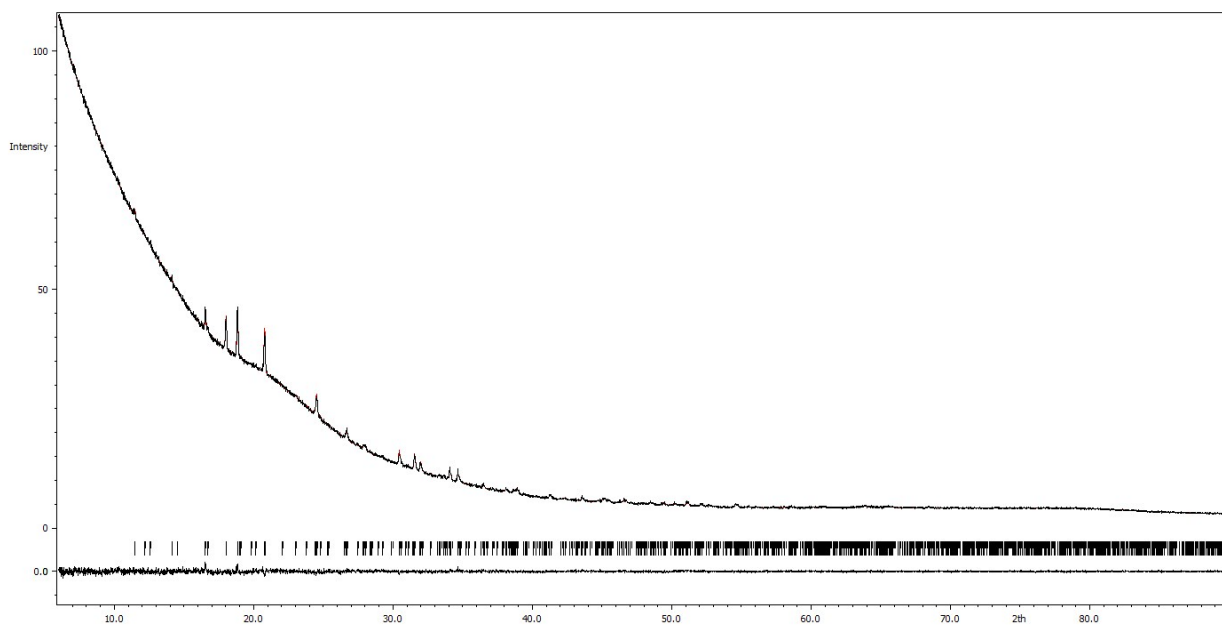


Figure S1. Rietveld refinement of PXRD ($\text{Cu K}\alpha$) data collected for $\text{CsSc}(\text{BH}_4)_4$ at room temperature, $wR_p = 1.17\%$, $R(\text{obs}) = 4.72\%$.

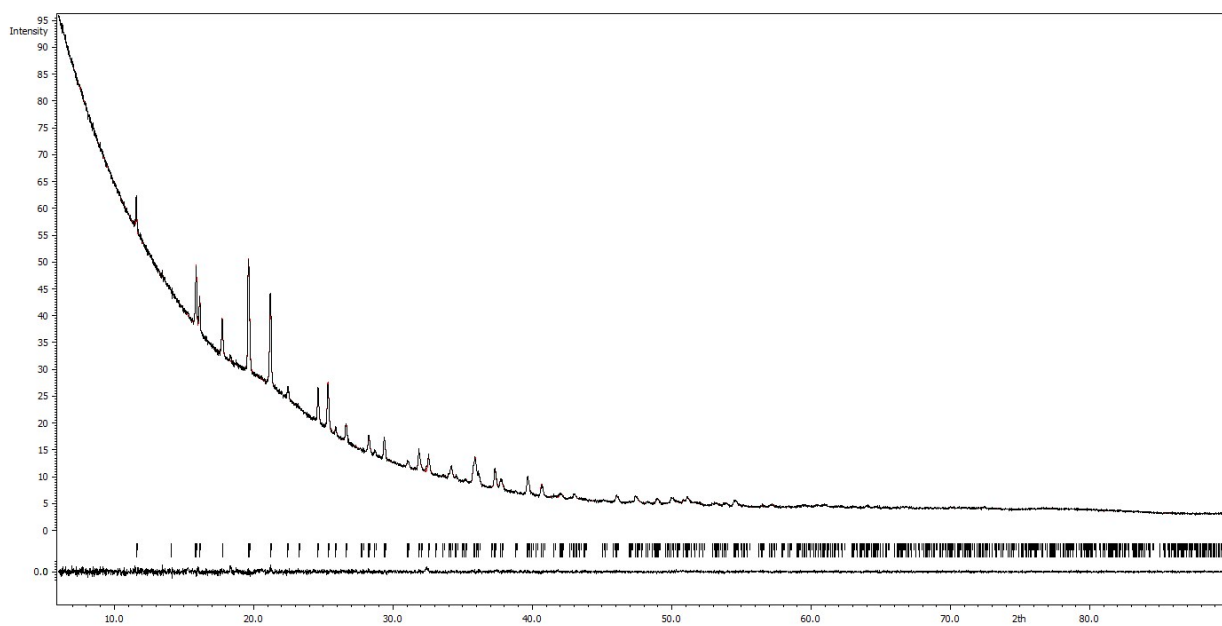


Figure S2. Rietveld refinement of PXRD ($\text{Cu K}\alpha$) data collected for $\text{RbSc}(\text{BH}_4)_4$ at room temperature, $wR_p = 1.23\%$, $R(\text{obs}) = 2.29\%$.

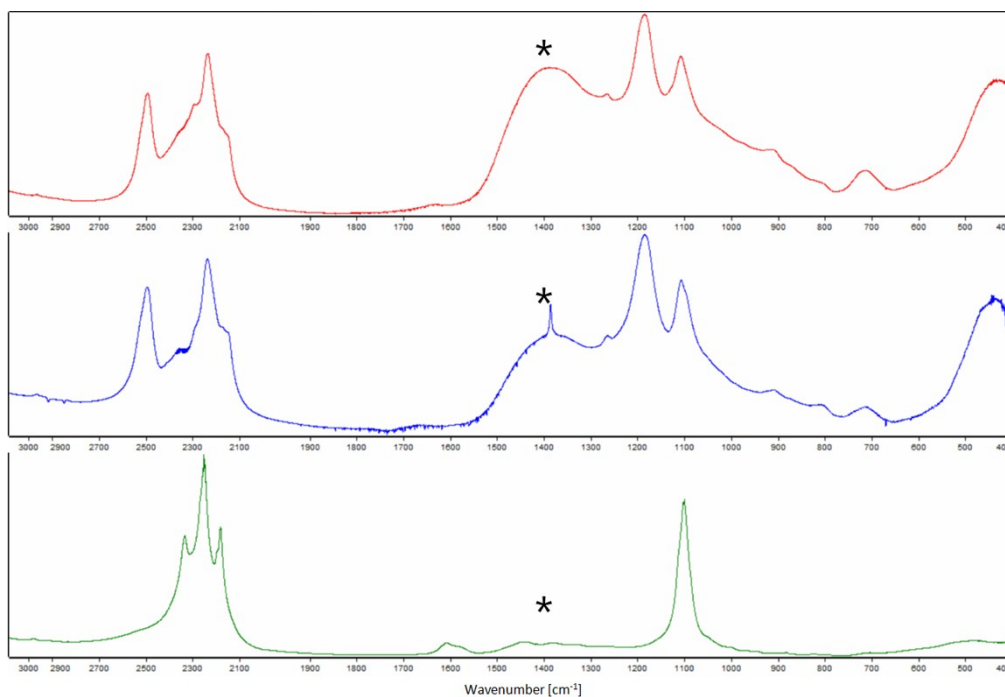


Figure S3. FTIR spectra of $\text{CsSc}(\text{BH}_4)_4$ obtained via mechanochemical (top) and solvent-mediated (middle) synthesis as well as of by-products of solvent-mediated synthesis (down, site **B**), * - background compensation error.

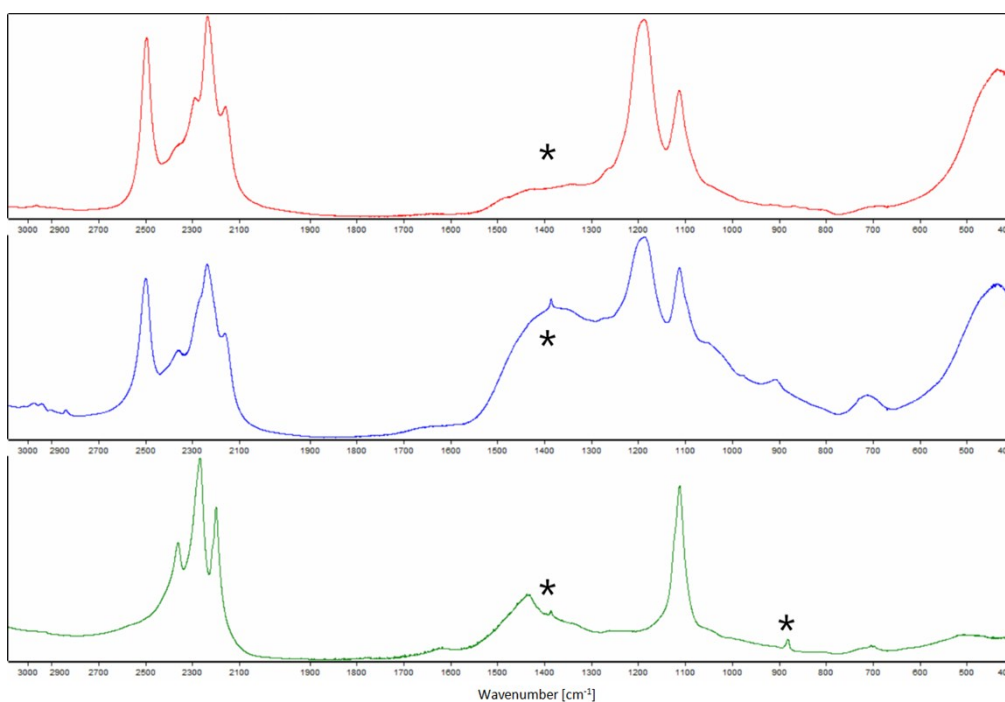


Figure S4. FTIR spectra of $\text{RbSc}(\text{BH}_4)_4$ obtained via mechanochemical (top) and solvent-mediated (middle) synthesis as well as of by-products of solvent-mediated synthesis (down, site **B**), * - background compensation errors.

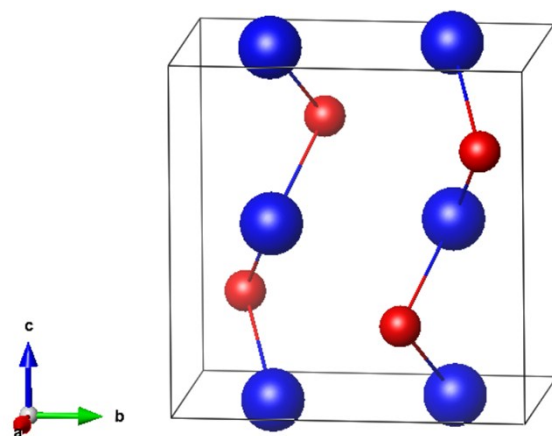


Figure S5. Sc-Rb zigzag lines along the *c*-axis in $\text{RbSc}(\text{BH}_4)_4$. Rb atoms in blue, Sc in red, Sc-Rb distance 4.487(5) Å.

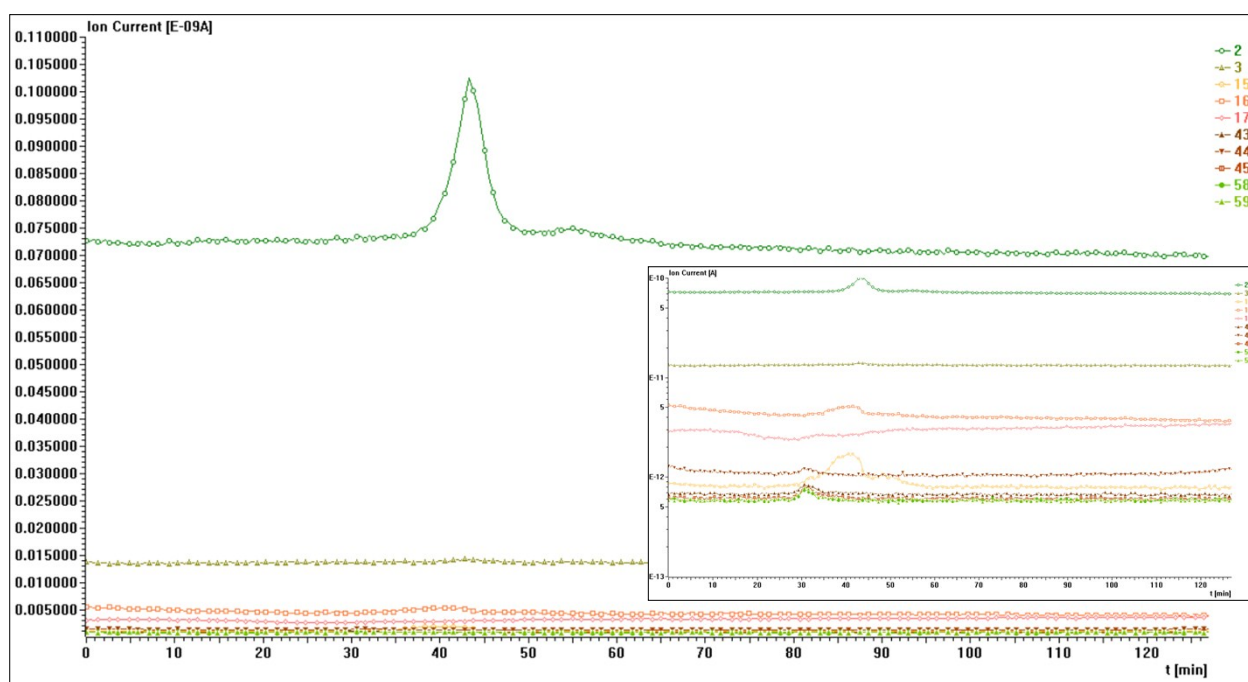


Figure S6. Mass spectrum of gaseous decomposition products of $\text{RbSc}(\text{BH}_4)_4$ obtained mechanochemically (inset: spectrum with logarithmic Ion current scale). Heating rate 5 °C/min, $t = 0$ corresponds to temperature 15 °C.

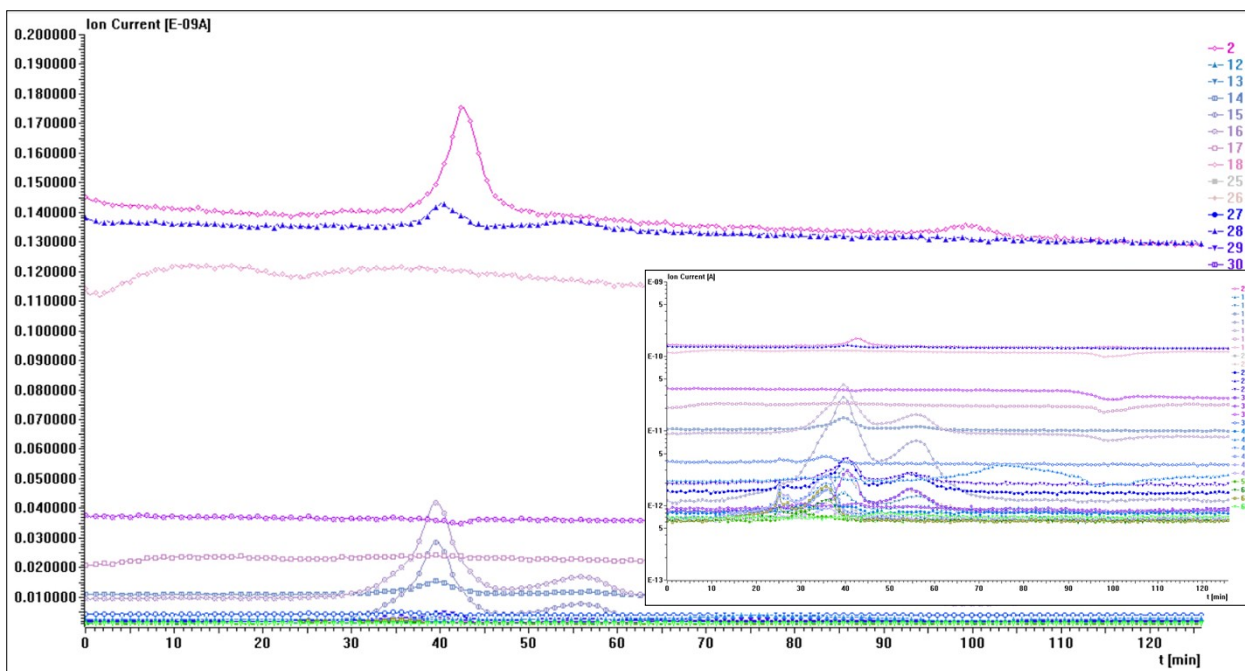


Figure S7. Mass spectrum of gaseous decomposition products of $\text{RbSc}(\text{BH}_4)_4$ obtained via DMS-mediated synthesis (inset: spectrum with logarithmic Ion current scale). Heating rate $5^\circ\text{C}/\text{min}$, $t = 0$ corresponds to temperature 20°C .

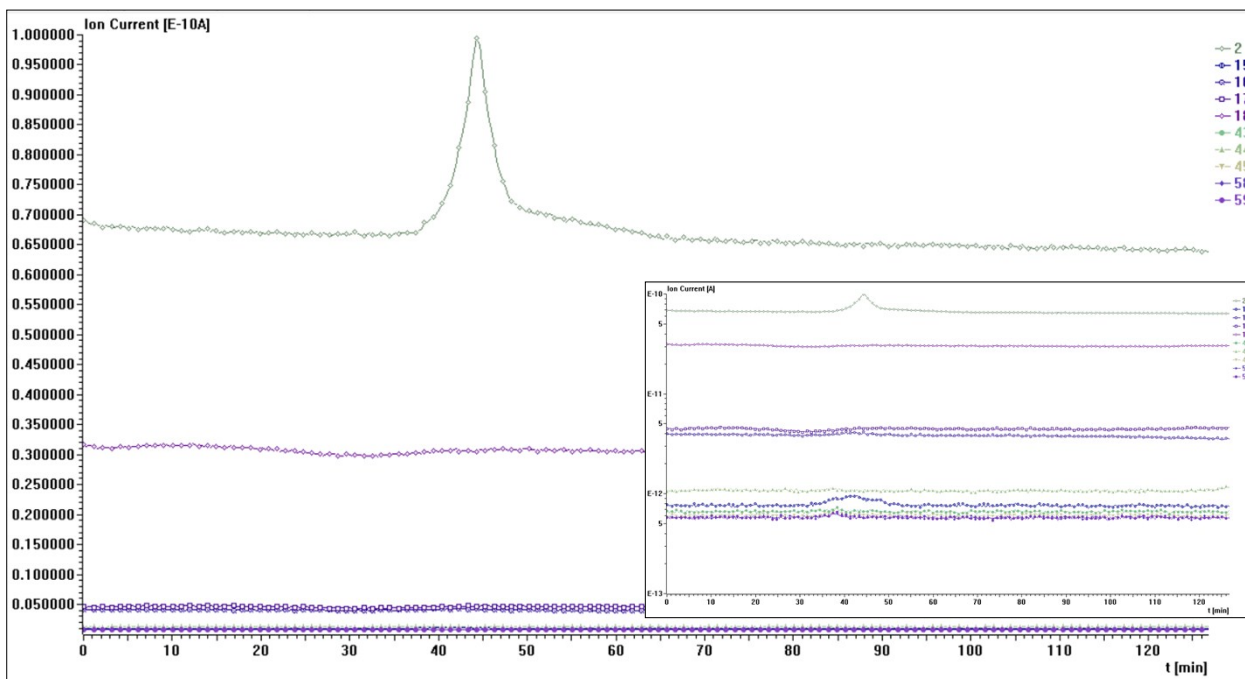


Figure S8. Mass spectrum of gaseous decomposition products of $\text{CsSc}(\text{BH}_4)_4$ obtained mechanochemically (inset: spectrum with logarithmic Ion current scale). Heating rate $5^\circ\text{C}/\text{min}$, $t = 0$ corresponds to temperature 15°C .

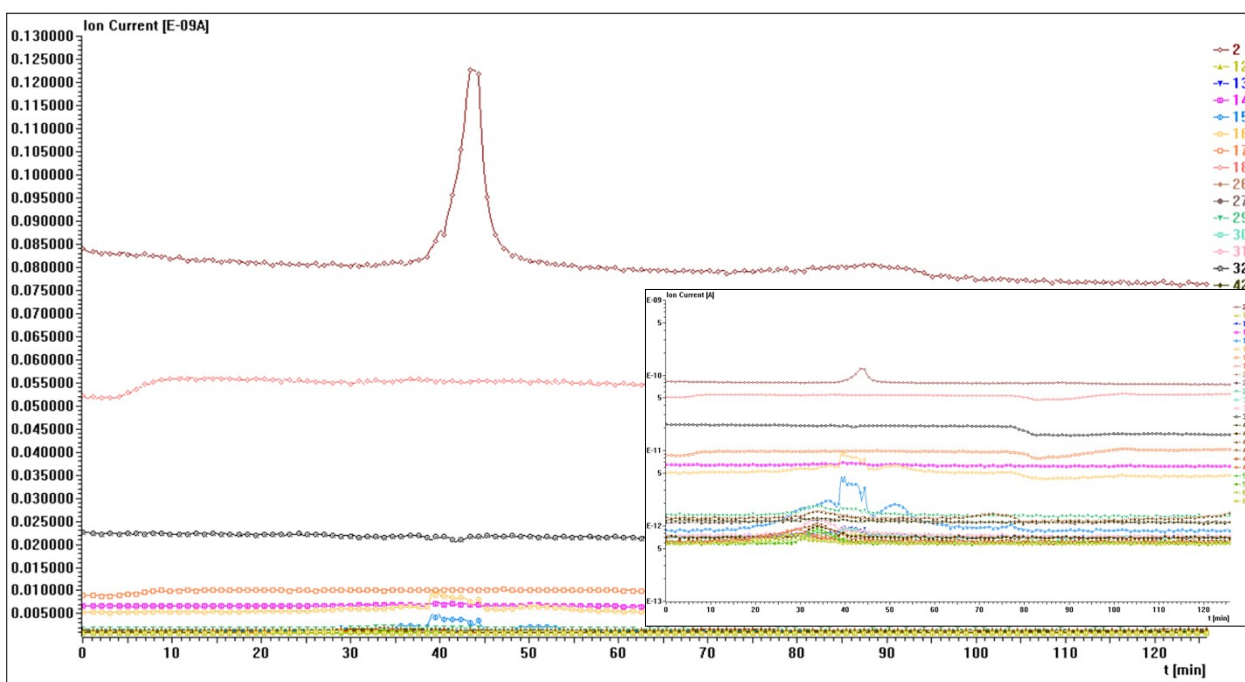


Figure S9. Mass spectrum of gaseous decomposition products of $\text{CsSc}(\text{BH}_4)_4$ obtained via DMS-mediated synthesis (inset: spectrum with logarithmic Ion current scale). Heating rate $5\text{ }^\circ\text{C}/\text{min}$, $t = 0$ corresponds to temperature $20\text{ }^\circ\text{C}$.

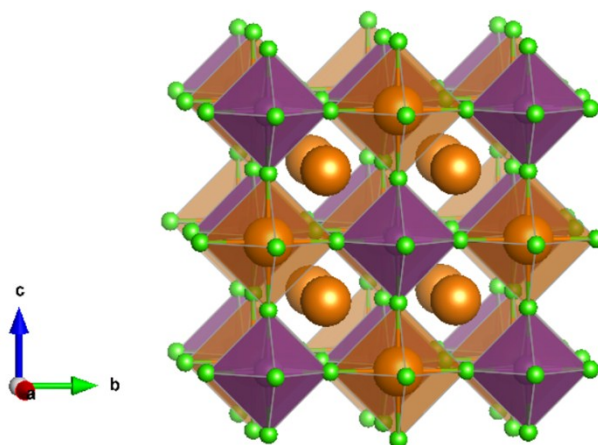


Figure S10. Crystal structure of M_3ScCl_6 , $\text{M}=\text{Rb}, \text{Cs}$ - the elpasolite-type structure. M atoms in orange, Sc - purple, Cl - green.

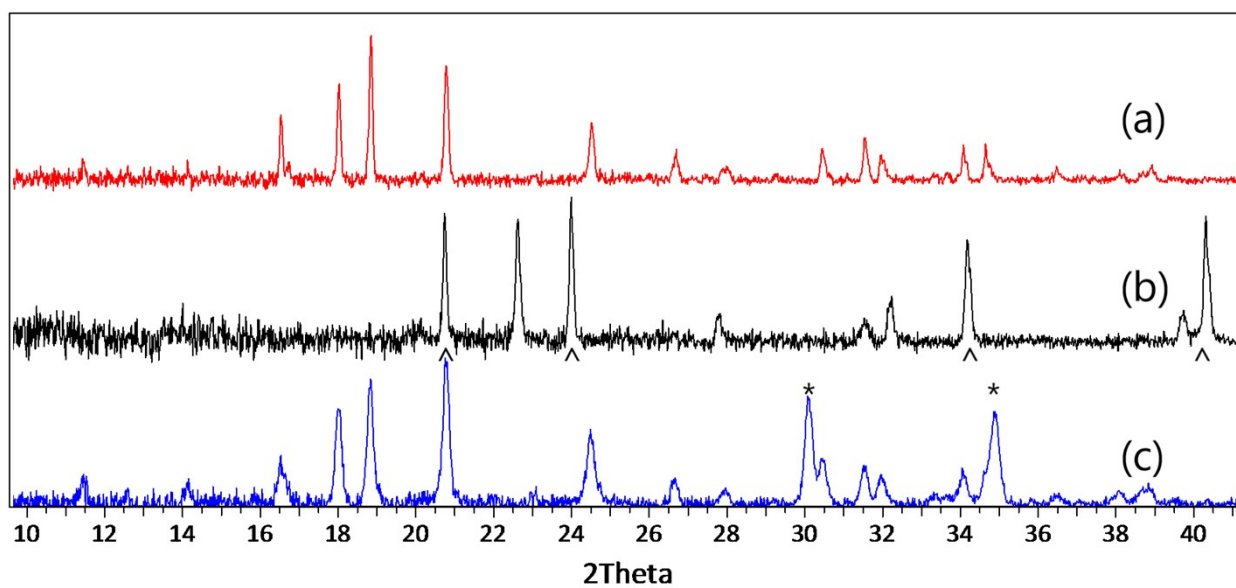


Figure S11. PXRD patterns of $\text{CsSc}(\text{BH}_4)_4$ samples obtained via the solvent-mediated (a) and the mechanochemical (c) synthesis and by-products of solvent-mediated synthesis (b), * - LiCl , ^ - CsBH_4 , unmarked - $\text{CsSc}(\text{BH}_4)_4$ or Cs_3ScCl_6 , respectively.

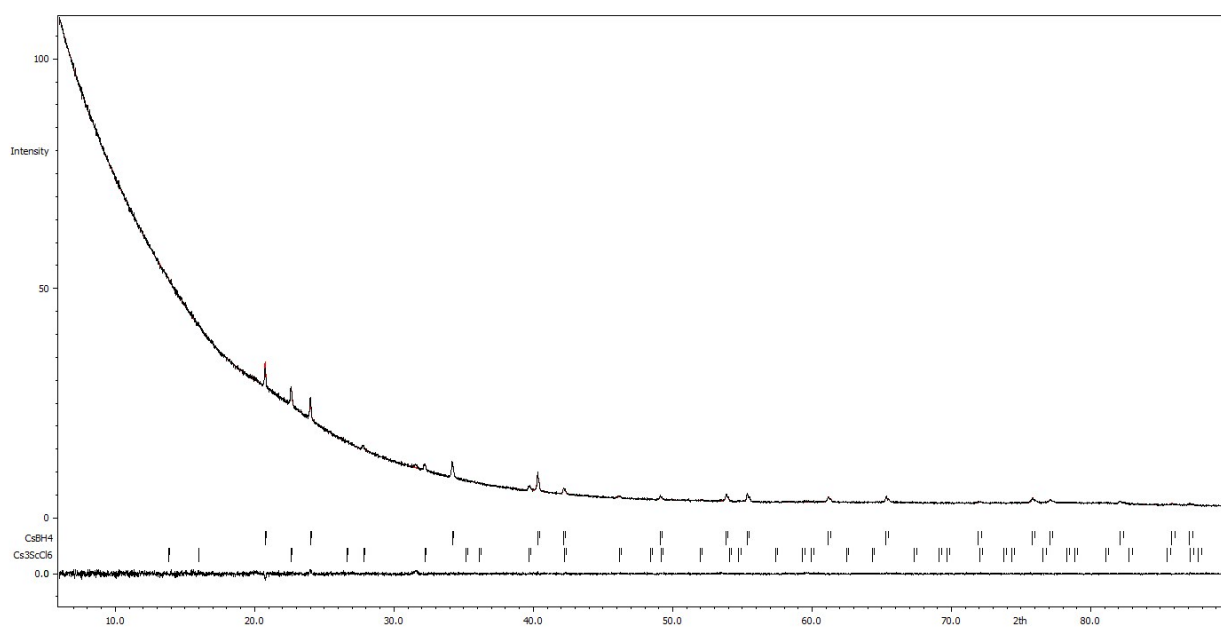


Figure S12. Rietveld refinement of PXRD ($\text{Cu K}\alpha$) data collected for Cs_3ScCl_6 sample at room temperature, $wRp = 1.20\%$, $R(\text{obs})_{\text{CsBH}_4} = 3.66\%$, $R(\text{obs})_{\text{Cs}_3\text{ScCl}_6} = 3.20\%$.

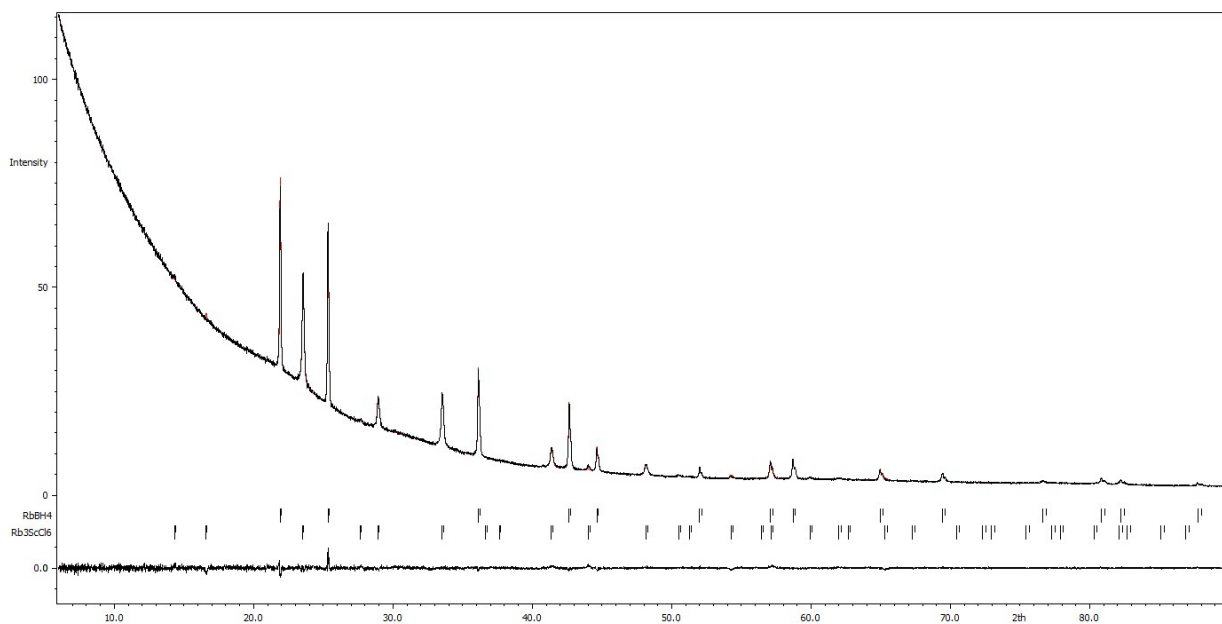


Figure S13. Rietveld refinement of PXRD (Cu K_{α}) data collected for Rb_3ScCl_6 sample at room temperature, $wRp = 1.48\%$, $R(obs)_{RbBH_4} = 2.57\%$, $R(obs)_{Rb_3ScCl_6} = 5.24\%$.

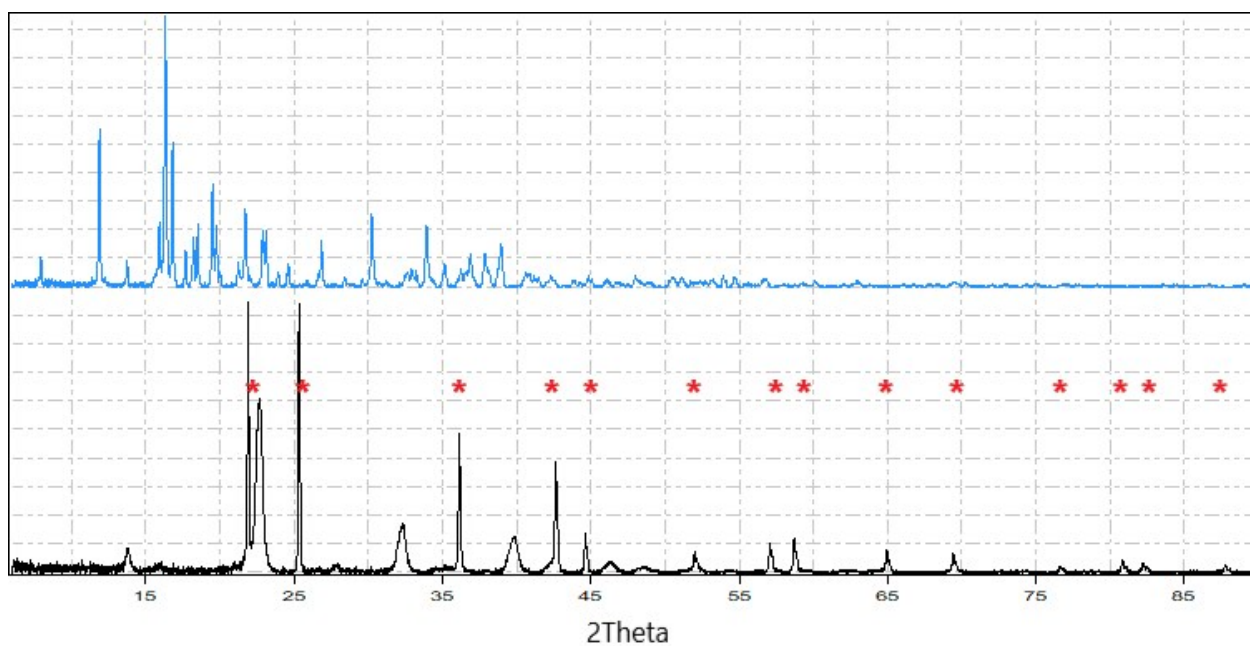


Figure S14. PXRD patterns of Rb-Y samples prepared via solvent-mediated method, site **A** - $Y(BH_4)_3 \cdot DMS$ (top), and site **B** - $RbBH_4$ (marked with *) and $ht-Rb_3YCl_6$ (bottom).

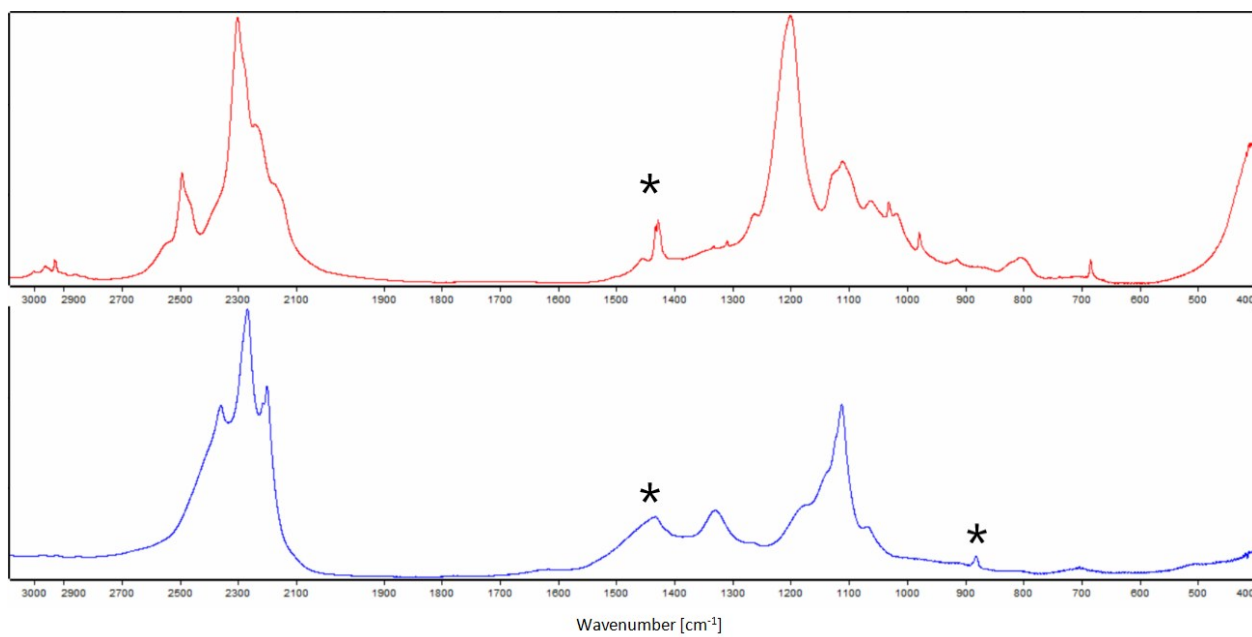


Figure S15. FTIR spectra of Rb-Y samples prepared via solvent-mediated method, site **A** - Y(BH₄)₃·DMS (top), and site **B** - RbBH₄ and ht-Rb₃YCl₆ (bottom), * - background compensation errors.

The structures of $\text{MSc}(\text{BH}_4)_4$ optimized computationally

RbSc(BH_4)₄

```
data_RbScCORRECTED_Geom800eV_6cores_NoCell
_audit_creation_date      2019-06-26
_audit_creation_method    'Materials Studio'
_symmetry_space_group_name_H-M  'PBCM'
_symmetry_Int_Tables_number  57
_symmetry_cell_setting    orthorhombic
loop_
_symmetry_equiv_pos_as_xyz
  x, y, z
  -x, -y, z+1/2
  -x, y+1/2, -z+1/2
  x, -y+1/2, -z
  -x, -y, -z
  x, y, -z+1/2
  x, -y+1/2, z+1/2
  -x, y+1/2, z
_cell_length_a           7.6514
_cell_length_b           11.1821
_cell_length_c           11.2443
_cell_angle_alpha        90.0000
_cell_angle_beta         90.0000
_cell_angle_gamma        90.0000
loop_
_atom_site_label
_atom_site_type_symbol
_atom_site_fract_x
_atom_site_fract_y
_atom_site_fract_z
_atom_site_U_iso_or_equiv
_atom_site_adp_type
_atom_site_occupancy
B1      B      0.23519  0.02670  -0.58184  0.02200  Uiso  1.00
H11     H      0.36413  0.04382  -0.64732  0.02700  Uiso  1.00
H12     H      0.27076  -0.02575  -0.49111  0.02700  Uiso  1.00
H13     H      0.17172  0.12656  -0.55910  0.02700  Uiso  1.00
H14     H      0.12514  -0.02621  -0.64381  0.02700  Uiso  1.00
H21     H      0.94449  0.21868  -0.83832  0.02700  Uiso  1.00
H32     H      0.22785  0.29877  -0.66164  0.02700  Uiso  1.00
Rb1     Rb     0.55522  0.25000  -0.50000  0.09067  Uani  1.00
Sc1     Sc     0.16021  0.13182  -0.75000  0.05967  Uani  1.00
B2      B      0.86828  0.17635  -0.75000  0.02200  Uiso  1.00
H22     H      0.71314  0.19760  -0.75000  0.02700  Uiso  1.00
H23     H      0.89853  0.06708  -0.75000  0.02700  Uiso  1.00
B3      B      0.32462  0.30552  -0.75000  0.02200  Uiso  1.00
H31     H      0.41624  0.21334  -0.75000  0.02700  Uiso  1.00
H33     H      0.41306  0.39492  -0.75000  0.02700  Uiso  1.00
```

CsSc(BH_4)₄

```
data_CsScGeom800eV_6cores_NoCell
_audit_creation_date      2019-06-26
_audit_creation_method    'Materials Studio'
```

```

_symmetry_space_group_name_H-M   'P21/C'
_symmetry_Int_Tables_number      14
_symmetry_cell_setting           monoclinic
loop_
_symmetry_equiv_pos_as_xyz
  x,y,z
  -x,y+1/2,-z+1/2
  -x,-y,-z
  x,-y+1/2,z+1/2
_cell_length_a                   9.5870
_cell_length_b                   10.7270
_cell_length_c                   12.2280
_cell_angle_alpha                90.0000
_cell_angle_beta                 126.3510
_cell_angle_gamma                90.0000
loop_
_atom_site_label
_atom_site_type_symbol
_atom_site_fract_x
_atom_site_fract_y
_atom_site_fract_z
_atom_site_U_iso_or_equiv
_atom_site_adp_type
_atom_site_occupancy
Cs22  Cs   0.82694  0.34270  0.75062  0.06900  Uiso  1.00
B1    B    0.21177  0.01695  0.27563  0.03500  Uiso  1.00
H2    H    0.23203  0.12082  0.32887  0.04200  Uiso  1.00
H3    H    0.15239 -0.05817  0.31159  0.04200  Uiso  1.00
H4    H    0.11686  0.03374  0.15052  0.04200  Uiso  1.00
H5    H    0.35660 -0.01335  0.30707  0.04200  Uiso  1.00
B6    B    0.59468  0.22457  0.38529  0.03500  Uiso  1.00
H7    H    0.53578  0.28562  0.27965  0.04200  Uiso  1.00
H8    H    0.74057  0.25675  0.47509  0.04200  Uiso  1.00
H9    H    0.48976  0.23768  0.41267  0.04200  Uiso  1.00
H10   H    0.58853  0.11248  0.35595  0.04200  Uiso  1.00
B11   B    0.13689  0.33158  0.11960  0.03500  Uiso  1.00
H12   H    0.20824  0.31906  0.24318  0.04200  Uiso  1.00
H13   H    0.03689  0.41819  0.07083  0.04200  Uiso  1.00
H14   H    0.25418  0.34173  0.10504  0.04200  Uiso  1.00
H15   H    0.06144  0.23137  0.06534  0.04200  Uiso  1.00
B16   B    0.33930  0.08443  0.04155  0.03500  Uiso  1.00
H17   H    0.39476  0.19319  0.07405  0.04200  Uiso  1.00
H18   H    0.35291  0.04517 -0.04403  0.04200  Uiso  1.00
H19   H    0.42198  0.02115  0.14752  0.04200  Uiso  1.00
H20   H    0.18734  0.08764  0.00469  0.04200  Uiso  1.00
Sc21  Sc   0.32111  0.16280  0.20685  0.04500  Uiso  1.00

```

Table S1. Comparison of the selected parameters for the experimental and computed structures.

MSc(BH ₄) ₄	Rb		Cs	
	experimental	DFT	experimental	DFT
Space group	<i>Pbcm</i>		<i>P2₁/c</i>	
Z	4		4	
a [Å]	7.6514(10)	7.6514	9.587(2)	9.5870
b [Å]	11.1821(14)	11.1821	10.727(3)	10.7270
c [Å]	11.2443(14)	11.2443	12.228(3)	12.2280
β [°]	90	90	126.351(3)	126.3510
V [Å ³]	962.1(2)	962.1	1012.8(5)	1012.8
Sc–H [Å]	2.255(8)	2.129–2.177	2.202(7)	2.143–2.184
M–Sc [Å]	4.487(4); 5.374–5.512(4)	4.334; 5.556–5.57462	4.788(11)–4.993(7); 5.685–5.787(8)	4.553–5.095; 5.594–5.974
Sc–B [Å]	2.360(8)	2.289–2.314	2.300(3)	2.289–2.303
M–B [Å]	3.494(7)– 3.806(6)	3.377–3.784	3.630(8)–4.165(11)	3.541–3.909

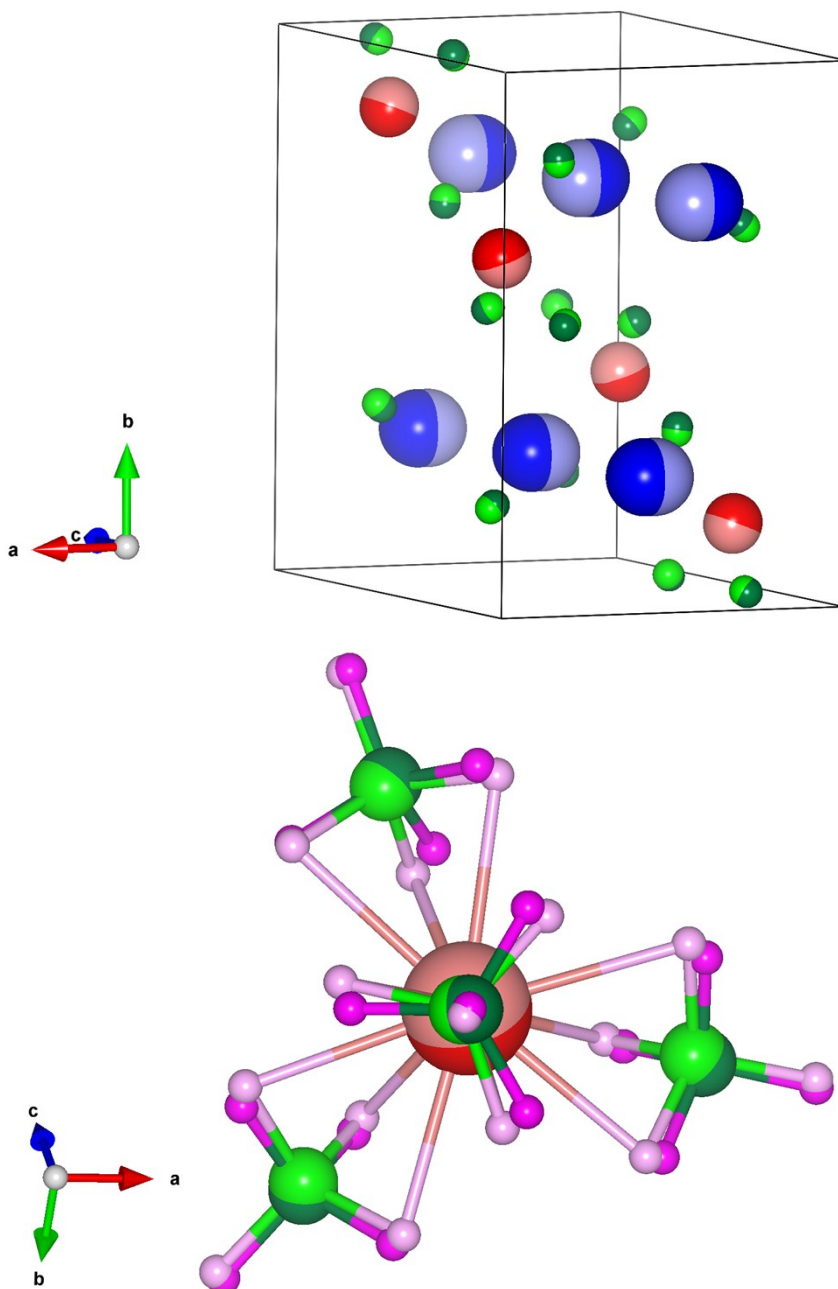


Figure S16. An overlay of the experimental (darker colors) and computationally optimized (brighter colors) structures of $\text{RbSc}(\text{BH}_4)_4$. Top – the sublattice of heavy atoms; bottom – the geometry of the $[\text{Sc}(\text{BH}_4)_4]^-$ complex anion.

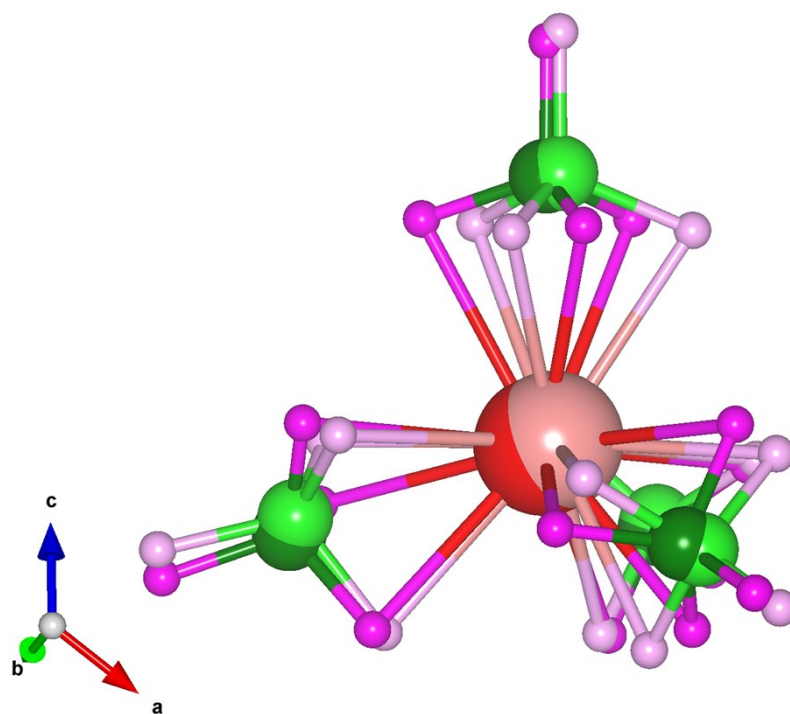
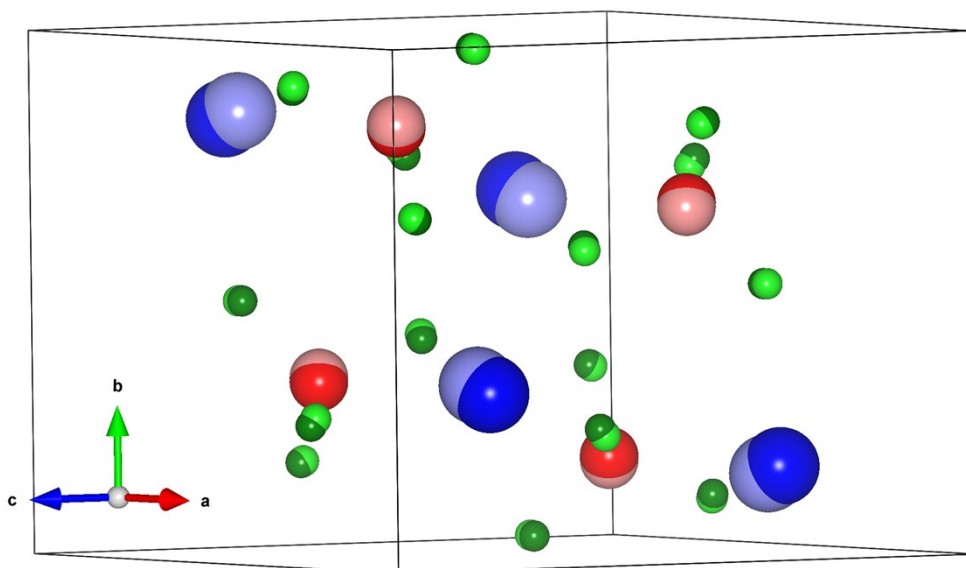


Figure S17. An overlay of the experimental (darker colors) and computationally optimized (brighter colors) structures of $\text{CsSc}(\text{BH}_4)_4$. Top – the sublattice of heavy atoms; bottom – the geometry of the $[\text{Sc}(\text{BH}_4)_4]^-$ complex anion.